Chapter 6

Heterotrophic prokaryotic growth and loss rates along a latitudinal gradient in the Northeast Atlantic Ocean

Kristina D. A. Mojica[1], and Corina P. D. Brussaard[1,2]

[1]Department of Biological Oceanography, Royal Netherlands Institute for Sea Research (NIOZ), P.O. Box 59, 1790 AB Den Burg, Texel, The Netherlands
[2]Department of Aquatic Microbiology, Institute for Biodiversity and Ecosystem Dynamics (IBED), University of Amsterdam, P.O. Box 94248, 1090 GE Amsterdam, The Netherlands

Abstract

The production and mortality of prokaryotes were assessed over a latitudinal gradient in the North Atlantic Ocean during summer stratification. Heterotrophic production was uncoupled from phytoplankton biomass and closely tied to nutrient availability suggesting nutrient limitation played an important role in regulating host production dynamics. Viruses were the dominate mortality factor regulating prokaryotic losses in the surface waters of the Northeast Atlantic Ocean. Wherein, lytic viral production was the favored life strategy for prokaryotic viruses in the mixed layer, independent of system trophic status, with rates ranging from 0.9 to 57.0 $x10^9$ viruses l^{-1} d^{-1}. Lytic VP in the surface waters was correlated to heterotrophic production and the nitrogen to phosphorus ratio. Lysogeny was important only within the deep chlorophyll maximum layer of oligotrophic stations wherein prophage induction decreased hyperbolically from 16.0 to 0.2 $x10^9$ viruses l^{-1} d^{-1} with latitude and Chl *a*. Our results suggest that inorganic nutrient limitation is an important factor regulating heterotrophic prokaryotic production, viral life strategy selection and lytic viral production in the North Atlantic Ocean. Moreover, the ratio of total mortality to heterotrophic production decreased over the latitudinal gradient signifying a gradual change from a system regulated by high turnover in regions of strong stratification to net heterotrophic production with reduced stratification.

Introduction

Prokaryotic viruses are abundant, diverse and pervasive components of marine systems (Suttle 2005; Angly et al. 2006). Viral lysis of microbes shunts matter and energy towards the particulate and dissolved organic matter pools and away from higher trophic levels and thus influences the structure of microbial food webs (Fuhrman 1999; Wilhelm and Suttle 1999). In addition, viral lysis releases cellular material rich in phosphorus and nitrogen compounds, providing substrate for heterotrophic prokaryotes, enhancing respiration and nutrient regeneration and stimulating primary production (Middelboe et al. 1996; Gobler et al. 1997; Middelboe and Jorgensen 2006; Sheik et al. 2014). The viral shunt thus plays an integral role in biogeochemical cycles of the ocean (Fuhrman 1999; Wilhelm and Suttle 1999; Brussaard et al. 2008).

Viral replication in prokaryotes largely occurs by either lytic or lysogenic infection, and the relative importance of these varies throughout the ocean (Payet and Suttle 2013). In the lytic cycle, viral replication proceeds immediately after infection and terminates with the lysis of the host, releasing viral progeny and host cell content into the surrounding water. Conversely, during lysogenic infection, the genetic material of temperate phages (prophage) is stably incorporated into the host genome, and the host continues to live and reproduce normally, transmitting the prophage vertically to daughter cells during each subsequent cell division. Hosts of temperate phages may benefit from association with lysogens, through protection against infection from homologous phages and through advantageous traits encoded in viral genomes (Chibani-Chennoufi et al. 2004; Weinbauer 2004; Gama et al. 2013). The few studies that have examined both viral life strategies, suggest that the relative importance of lysogenic and lytic infection is related to trophic status of the system, which has lead to the theory that lysogeny represents a survival strategy under conditions of low host productivity and abundance (Payet and Suttle 2013; Mojica and Brussaard 2014).

Bottom up resource availability of dissolved organic carbon (DOC) is thought to be the primary factor regulating the activity of heterotrophic prokaryotes in much of the world's oceans (Kirchman 1990; Carlson and Ducklow 1996; Church et al. 2000). Although DOC regulates heterotrophic prokaryotic activity, studies indicate that in oligotrophic regions heterotrophic prokaryotic growth can be limited by N and/or P (Cotner et al. 1997; Rivkin and Anderson 1997; Mills et al. 2008). Therefore, heterotrophic prokaryotic biomass and activity may be related to the nutrient supply and thus to water column stability (Gasol et al. 2009).

The North Atlantic Ocean is key to ocean circulation and stores about 23% of the global ocean anthropogenic CO_2 (Sabine et al. 2004). The northeastern basin provides a meridional gradient in stratification, with permanent stratification in the subtropics and seasonal stratification in the temperate zones (Talley et al. 2011; Jurado et al. 2012a). Vertical stratification suppresses turbulence and reduces the mixed layer depth, and restricts the flow of nutrients from depth. Strong and prolonged stratification often leads to oligotrophication of surface waters as nutrient become depleted due to utilization (Behrenfeld et al. 2006; Huisman et al. 2006; Hoegh-Guldberg and Bruno 2010). Moreover, as a consequence of global warming, oligotrophic areas (i.e., defined as areas below 0.07 μg Chl l^{-3}) are expected to expand in the future (Polovina et al. 2008). Therefore, the Northeast Atlantic provides an ideal area to study the relative contribution of lytic and lysogenic viral infection in a system governed by seasonal stratification.
Here we assess (1) viral induced mortality of prokaryotes relative to grazing over a latitudinal gradient across the North Atlantic Ocean during summer stratification, (2) the proportion of lytic and lysogenic viral infection and (3) discuss the results in terms implications for carbon cycling.

Materials and Methods

Sampling and physicochemical parameters

In July-August of 2009, 32 stations were sampled along a latitudinal gradient in the Northeast Atlantic Ocean during the shipboard expedition of STRATIPHYT which took place onboard othe R/V Pelagia (Fig. 1). Along the transect, the water column was stratified with relatively consistent and shallow mixed layer (ML) depths ranging from 18 - 46 m (Jurado et al. 2012b). Water samples for dissolved inorganic nutrients, bacterial and viral abundances were collected from at least 10 separate depths at each station using 24 plastic samplers (General Oceanics type Go-Flow, 10 liter) mounted on an ultra-clean (trace-metal free) system consisting of a fully titanium sampler frame equipped with CTD (Seabird 9+; standard conductivity, temperature and pressure sensors) and auxiliary sensors for chlorophyll autofluorescence (Chelsea Aquatracka Mk III), light transmission (Wet-Labs C-star) and photosynthetic active radiation (PAR; Satlantic). Samples were collected inside a 6 m clean container. Data from the chlorophyll autofluorescence sensor were calibrated against HPLC data according to van de Poll et al. (2013) (van

de Poll et al. 2013). At 16 stations along the cruise transect (Fig. 1), samples for heterotrophic prokaryote production, virus mediated mortality and protist grazing of prokaryotes were collected from the mixed layer (ML) and, where present, the deep-chlorophyll maximum (DCM; defined by the presence of a subsurface peak in the vertical profile of Chl *a* autofluorescence).

Methods and data for temperature eddy diffusivity (K_T), euphotic depth (Z_{eu}), and dissolved inorganic nutrients have been discussed previously (Jurado et al. 2012b; Mojica et al. 2015). In short, K_T (referred to here as the vertical mixing coefficient) was derived from temperature and conductivity microstructure profiles measured using a SCAMP (Self Contained Autonomous Microprofiler), deployed at 14 stations and down to 100 m depth. For the additional stations and depths, data were interpolated using the spatial kriging function 'krig' executed in R using the 'fields' package (Furrer et al. 2012). Interpolated K_T values were bounded below by the minimum value measured; the upper values were left unbounded. This resulted in estimated K_T values which preserved the qualitative pattern and range of values reported by Jurado et al. (Jurado et al. 2012b). Brunt-Väisälä frequency (N^2), was used to quantify the strength of stratification and was determined from CTD data processed with SBE Seabird software according to the Fofonoff adiabatic leveling method (Bray and Fofonoff 1981).

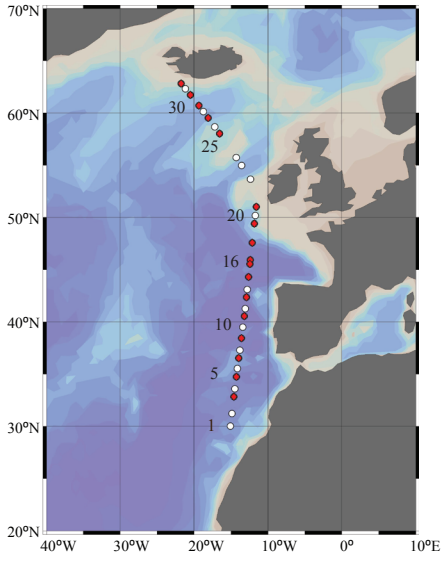

Figure 1. North-south gradient across the Northeast Atlantic Ocean. Bathymetric map depicting stations sampled during the summer STRATIPHYT. Mortality assays to determine viral lysis and microzooplankton grazing rates were performed at stations indicated by the red. Figure was prepared using Ocean Data View version 4 (Schlitzer 2002).

Samples for dissolved inorganic phosphate (PO_4^{3-}), ammonium (NH_4^+), nitrate (NO_3^-), and nitrite (NO_2^-) were gently filtered through 0.2 µm pore size polysulfone Acrodisk filters (32 mm, Pall Inc.), after which samples were stored at -20°C until analysis. Dissolved inorganic nutrients were analyzed onboard using a Bran+Luebbe Quaatro AutoAnalyzer for dissolved orthophosphate (PO_4^{3-}) (Murphy and Riley 1962), inorganic nitrogen (nitrate + nitrite: NO_x) (Grasshoff 1983) and ammonium (NH_4^+) (Koroleff 1969; Helder and de Vries 1979). Detection limits were 0.10 µM for NO_x, 0.028 µM for PO_4^{3-} and 0.09 µM for NH_4^+. The ratio of nitrogen to phosphorus (N:P) was then calculated as the sum of NO_x and NH_4^+ divided by PO_4^{3-}. For the individual nutrients, the flux at the euphotic zone depth ($Z_{eu}N$) was calculated according to $\varphi(Z_{eu}) = -K_T(z)(\partial N/\partial z)|_{Zeu}$, where N represents the individual nutrient and z stands for depth. Z_{eu} was calculated based on the light attenuation coefficient (K_d) and was defined as the depth at which irradiance was 0.1% of the surface value.

Microbial abundances

Prokaryotes and viruses were enumerated using Becton-Dickinson FACSCalibur flow cytometer (FCM) equipped with an air-cooled Argon laser with an excitation wavelength of 488 nm (15 mW) according to Marie et al. (1999), with modifications according to Mojica et al. (2014). Briefly, samples were fixed with 25% glutaraldehyde (EM-grade, Sigma-Aldrich, Netherlands) at a final concentration of 0.5% for 15 - 30 min at 4°C, flash frozen and stored at -80°C until analysis. Thawed samples were diluted using TE buffer, pH 8.2 (10 mM Tris-HCL, 1 mM EDTA; Roche, Germany). Prokaryote samples were stained in the dark at room temperature for 15 min using SYBR Green I at a final concentration of 1×10^{-4} of the commercial stock. Virus samples were stained by heating in the dark at 80°C for 10 min in the presence of the nucleic acid-specific green fluorescence dye SYBR Green I at a final concentration of 0.5×10^{-4} of the commercial stock concentration (Life Technologies, Netherlands). Trigger for analysis was set on green fluorescence and the obtained list-mode files were analyzed using the freeware CYTOWIN (Vaulot 1989).

Heterotrophic nanoflagellates (HNF) were enumerated by epifluorescence microscopy. Briefly, 20 ml of seawater was fixed to a 1% final concentration (10% working stock, Sigma Aldrich) and filtered onto 0.2 µm black polycarbonate filter (25 mm, Whatman). Samples were then stained using 4'6-diamidino-2-phenylindole dihydrochloride (DAPI) (5 mg ml^{-1}, Sigma-Aldrich) at a final concentration of 1 µg ml^{-1} and stored at -20°C. A minimum of 75 fields and 100 HNF in total were then

counted using a Zeiss Axiophot epifluorescence microscope equipped with BP 365, FT395 and LP397 excitation filters.

Viral mediated mortality

Viral production (VP) was determined according to Winget et al. (2005). At *in situ* temperature and under low light conditions, a 600 ml whole seawater sample was reduced to approximately 100 ml by recirculation over a 0.22 µm-pore-size polyether sulfone membrane (PES) tangential flow filter (Vivaflow 50; Sartorius stedim biotech) at a filtrate discharge rate of 40 ml min^{-1}. Five hundred milliliters of virus-free water (generated by 30-kDa ultrafiltration Vivaflow 200, PES membrane; Sartorius stedim biotech) was then added and the washing procedure was repeated an additional 2 times. On the final flush, the volume was reduced a final time to approximately 50 ml and the filter was slowly back-flushed to obtain the 50 ml volume remaining in the system. The sample was then topped up with virus-free water (500 ml) and aliquoted into six 50 ml polycarbonate Greiner tubes. Triplicate samples were used to determine lytic VP, and triplicates for prophage induction using Mytomycin C (Sigma-Aldrich; 1 µg ml^{-1} final concentration) (Paul and Weinbauer 2010). Untreated whole seawater was also aliquoted into three 50 ml polycarbonate tubes in order to provide an estimate of PP_{net}. One milliliter subsamples for viral and prokaryotic abundance were taken at the start of the incubation (T_0), after which the samples were incubated in darkness at *in situ* temperature and sub-sampled every 3 h for a total of 12 - 24 h.

Production rate of new viruses was determined for each replicate from the slope of a first-order regression of viral concentration over time (Wilhelm et al. 2002). Prophage induction was calculated as the difference between virus counts in unamended samples (lytic VP) and virus counts in those to which Mitomycin C was added. The *in situ* VP rate was determined by correcting the experimental VP rate by the prokaryotic loss factor (Winget et al. 2005). Estimates for daily virus-mediated mortality (VMM) expressed in cells l^{-1} d^{-1} were calculated by dividing lytic VP by a burst size of 20 (Parada et al. 2006). Estimates of VMM, in terms of organic carbon released by viral lysis, were obtained by multiplying the VMM by the oceanic bacterial carbon conversion factor of 12.4 fg $cell^{-1}$ (Fukuda et al. 1998).

Protist mediated mortality

Protistian grazing rates of prokaryotes were determined using fluorescently labeled natural bacteria (FLP) according to the procedure described by Sherr and Sherr

(1987). One liter natural whole water samples (polycarbonate bottles) were given FLP at approximately 10% of the natural concentration (FLP stock contained 5 x 10^7 ml^{-1}, stored at -20°C until use). Immediately after addition, a 20 ml subsample (T_0) was then taken and fixed with 10% glutaraldehyde (1% final concentration; EM-grade, Sigma-Aldrich, Netherlands). The sample was then filtered onto a 0.2 µm pore-size black polycarbonate filter (25 mm, Whatman) and stored at -20°C until analysis. The incubation bottles were closed such that no air was trapped inside, mounted on a slow rotating (0.5 rpm) plankton wheel, and incubated under *in situ* light and temperature. After 24 h incubation, a 20 ml subsample was taken and treated as previously described. The estimation of grazing rates (d^{-1}) were determined as the natural log of the abundance of FLP in the T_{24} sample divided by the abundance of FLP in the T_0 sample. Protist mediated mortality (PMM) was calculated as $PMM = PA_0 \times (e^{rt}-1)$, where PA_0 is the abundance of protists and r equals the grazing rate obtained from FLP experiments.

Heterotrophic prokaryotic production

Heterotrophic prokaryotic production was determined from leucine incorporation rates (PP_L) according to Simon and Azam (1989). Ten-milliliter seawater samples were taken in triplicate. One sample was used as a control to which 0.5 ml formaldehyde (37%; Sigma-Aldrich) was added in order to kill the prokaryotes. Thirty µl [3H]leucine (specific activity, 139 Ci $mmol^{-1}$; Amersham) was added to each sample, equivalent to 50 microCurie per vial, and incubated in the dark at *in situ* temperature for 2 h. Samples were then fixed with 0.5 ml formaldehyde (37%; Sigma-Aldrich) and filtered onto 0.2 µm polycarbonate filters (25 mm, Whatman). Filters were washed twice by addition of 5% chilled trichloroacetic acid (TCA) for 5 min and then transferred to scintillation vials and stored at -80°C until analysis. Prior to analysis, 8 ml of scintillation cocktail (Filter-Count LCS cocktail; PerkinElmer) was added and left for 6 h. Samples were analyzed on a LKB WALLAC 1211 Rackbeta liquid scintillation counter. PP_L in terms of organic carbon produced was calculated assuming a carbon to protein ration of 0.86 and an isotope dilution factor of 2 (Simon and Azam 1989). Heterotrophic prokaryotic biomass production was converted to cell concentrations by dividing by the average carbon content of oceanic bacteria of 12.4 fg C $cell^{-1}$ (Fukuda et al. 1998).

PP_L is presumed to measure 'gross production' as the incubation period is short relative to prokaryotic growth and mortality (i.e., a day or longer) (Kirchman 2001). However, taking into account that generally no steps are taken to exclude

mortality, it is likely that losses are incorporated into the PP_L measurements. Heterotrophic prokaryotic production has been shown to be reduced up to 2-fold in the presence of viruses compared to incubations without viruses (Middelboe 2000). Net prokaryotic production (PP_{net}) determined by the increase in prokaryote abundance in unamended seawater over time was higher than the PP_L in more than half of the total paired samples (Table S1). One possibility is that PP_L could have been underestimated, as incubations were carried out in the dark, due to significant contributions of photoheterotrophs (i.e., aerobic anoxygenic phototrophs (AAP) or proteorhodopsin (PR) containing bacteria to prokaryotic abundance (Michelou et al. 2007; Campbell et al. 2008; Gomez-Consarnau et al. 2010). However, in all cases, rates of VMM and PMM were higher than PP_L (Table S1) and therefore it is more likely that PP_L represented net production. In order to account for this we calculated gross production (PP_{gross}) by correcting for losses due to viral lysis and grazing (assuming the rate of mortality in the samples was equivalent to those measured by the mortality assays and a 30% growth efficiency for grazing, i.e., 30% of carbon grazed was retained on filter) (Fenchel and Finlay 1983; Straile 1997). Therefore, $PP_{gross} = PP_L +$ lytic VMM+ [(0.3) x PMM]. Total available carbon (TAC) was then calculated as the sum of prokaryotic standing stock (PA) and production, i.e., PP_L for minimal TAC (TAC_{min}) and PP_{gross} for maximal TAC (TAC_{max}).

Statistical analysis

Statistical analysis was performed using the R statistical software (R Development Core Team 2012). Potential relationships between microbial abundances, production, mortality and environmental parameters were examined by Spearman rank correlation coefficients. Probability values were adjusted with Holm correction of multiple hypothesis testing using the corr.p function of psych (Revelle 2014). Analysis was performed on data as a whole (n = 25), but also separately according to depth layers; ML (n = 20) and DCM (n = 5).

Table 1. Location, physicochemical characteristics and Chl a autofluorescence of water sampled in the North Atlantic for heterotrophic prokaryotic production, viral production and grazing experiments. Abbreviations for depth layer are mixed layer (ML) and deep chlorophyll maximum (DCM).

Station	Latitude (°N)	Longitude (°E)	Depth (m)	Depth Layer	Z_{eu} (m)	Temperature (°C)	Salinity	NO_3^- (µM)	PO_4^{3-} (µM)	NH_4^+ (µM)	Chl *a* (µg l^{-1})
3	32.825	-14.589	15	ML	138	22.8	36.9	0.05	0.00	0.08	0.03
			60	DCM		18.1	36.5	0.07	0.00	0.06	0.24
5	34.720	-14.258	15	ML	119	22.3	36.7	0.00	0.01	0.10	0.04
			85	DCM		16.1	36.3	0.00	0.03	0.16	0.28
7	36.526	-13.934	15	ML	84	20.6	36.2	0.00	0.00	0.06	0.04
9	38.424	-13.586	15	ML	111	21.1	36.4	0.04	0.02	0.06	0.05
			75	DCM		14.9	36.1	1.32	0.13	0.18	0.29
11	40.528	-13.191	15	ML	96	19.8	36.0	0.00	0.01	0.06	0.06
13	42.337	-12.884	15	ML	99	18.7	35.8	0.05	0.03	0.00	0.04
			47	DCM		14.7	35.8	0.09	0.05	0.00	0.55
15	44.283	-12.605	15	ML	122	18.4	35.8	0.05	0.03	0.06	0.05
			60	DCM		14.4	35.8	2.05	0.17	0.07	0.62
16	45.917	-12.363	10	ML	86	16.9	35.6	0.10	0.04	0.04	0.51
18	47.569	-12.110	25	ML	88	16.6	35.7	0.07	0.05	0.11	0.46
19	49.382	-11.829	15	ML	115	15.8	35.5	1.15	0.12	0.31	0.22
19	49.382	-11.829	30	ML		15.7	35.5	1.29	0.16	0.39	0.30
21	51.000	-11.567	15	ML	115	15.9	35.5	1.15	0.15	0.39	0.23
25	58.002	-16.516	10	ML	43	13.5	35.3	1.18	0.11	0.09	1.45
27	59.499	-18.067	20	ML	41	14.0	35.2	2.08	0.18	0.19	1.09
29	60.684	-19.339	10	ML	49	13.1	35.3	2.00	0.19	0.17	0.94
30	61.715	-20.489	15	ML	48	13.1	35.2	1.38	0.15	0.33	1.08
32	62.800	-21.736	10	ML	38	12.8	35.3	1.52	0.14	0.64	1.21

Results

Study site

Temperature, salinity and density showed clear vertical and latitudinal gradients (Table 1, Fig. S1A-C). In accordance with strong vertical stratification, the upper water column was characterized by low K_T and relatively high N^2 (Fig. S1D, E and Table S2). Moreover, the southern region (30 - 45°N; stations 3 - 15) was classified as oligotrophic based on ML concentrations of $NO_3^- \leq 0.13$ µM and $PO_4^{3-} \leq 0.03$ µM (van de Poll et al. 2013), and Chl $a \leq 0.07$ µg l^{-1} (Polovina et al. 2008). In the northern half (46 - 63°N; stations 16 - 32), inorganic nutrient concentrations within the ML were on average 1.4±0.8 µM NO_3^- and 0.14±0.06 µM PO_4^{3-}, with highest concentrations north of 58°N (stations 25 - 32). In the ML, significant correlations were found between N:P and NH_4^+, NO_2^- (positive) and $Z_{eu}PO_4$ (negative; Table S3). Chl *a* in the ML was in turn positively correlated to N:P (and NH_4^+, NO_2^-

and negatively with $Z_{eu}PO_4$; Table S3) and average Chl *a* concentration increased to a maxima of 1.1±0.3 μg l^{-1} in the north (Table 1 and Fig. S1J). In the DCM (oligotrophic southern stations), K_T increased significantly with latitude (positively related to NO_3^- and PO_4^{3-}), and N^2 was negatively related to NO_2^-, $Z_{eu}NO_3$ and N:P (Table S4. Fig. S1D). N:P in the DCM was positively associated with NO_2^- and $Z_{eu}NO_3$. Chl *a* in the DCM increased significantly with latitude (positively related to K_T, NO_3^- and PO_4^{3-}) from 0.24 at station 3 to 0.62 μg l^{-1} at station 15 (Table 1 and S4, Fig. S1J).

Microbial abundances

Prokaryotic abundance (PA) in the ML was on average 6.4±1.5 x10^8 prokaryote l^{-1} until 58°N, above which concentrations increased to 22±0.8 x10^8 l^{-1} (Fig. 2A). Similar to their numerically dominate hosts, viral abundances (VA) were also lowest in the ML of oligotrophic south (average 8.0±2.9 x10^9 l^{-1}; Fig. 2B), however, VA increased earlier (~45°N) and remained relatively stable until 63°N with an average abundance of 24±0.9 x10^9 l^{-1}. The average virus to prokaryote ratio (VPR) in the ML increased from 13±5 in the most southern section of the transect to 26±9 midway through before declining again to 14±7 in the most northern stations (Table 2). HNF abundances in the ML were lowest in the most southern stations (< 40°N, averaging 3.5±1.0 x 10^5 l^{-1}). Highest abundances of 16 x10^5 were found near the DCM of stations 11 - 18 (40 - 47°N). North of this region, HNF in the ML averaged 9.6±2.3 x10^5 l^{-1}.

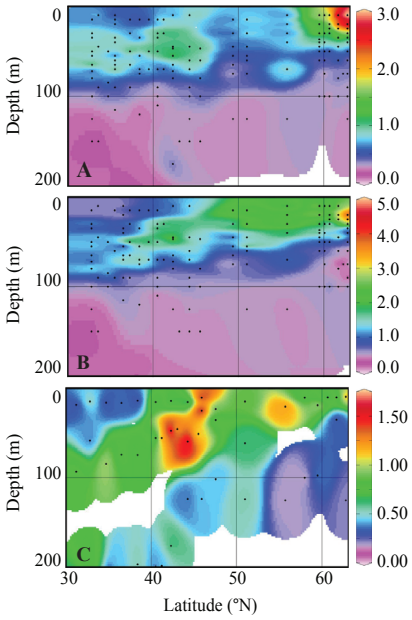

Figure 2. Biogeographical distributions of (**A**) prokaryotes (x10^{9} l^{-1}), (**B**) viruses (x10^{10} l^{-1}), and (**C**) heterotrophic nanoflagellates (x10^{6} l^{-1}) across the Northeast Atlantic Ocean obtained during the STRATIPHYT cruise. Black dots indicate sampling points. Graphs were prepared with Ocean Data View version 4 (Schlitzer 2002).

PA in the ML was significantly correlated to Chl *a* (Table S5). The positive correlation to NO_2^- and negative correlation to $Z_{eu}PO_4$ was most likely an indirect effect due to the high correlation of these variables with Chl *a* (Table S3 and S4). Viral abundance (VA) was tightly associated to their numerically dominate hosts (PA) (Table S5 and S6). However contrary to PA, VA in the ML was positively correlated to latitude and negatively with temperature and salinity (Table S5). VPR in the ML was inversely correlated to Chl *a*, explaining the relationship with $Z_{eu}PO_4$, NH_4^+ and N:P that were each associated to Chl *a* (Table S3 and S5).

Table 2. Heterotrophic nanoflagellates (HNF) abundance, prokaryotic abundance (PA), viral abundance (VA) and virus to prokaryote ratio (VPR) in stratified waters along a south-north transect in the Northeast Atlantic. Abbreviations for depth layer are mixed layer (ML) and deep chlorophyll maximum (DCM). n.d. = not determined.

Station	Latitude (°N)	Longitude (°E)	Depth (m)	Depth Layer	HNF ($x10^5$ l^{-1})	PA ($x10^8$ l^{-1})	VA ($x10^9$ l^{-1})	VPR
3	32.825	-14.589	15	ML	5.2	7.2	5.6	8
			60	DCM	3.8	11.2	10.5	9
5	34.720	-14.258	15	ML	3.0	7.7	7.4	10
			85	DCM	9.7	7.8	13.3	17
7	36.526	-13.934	15	ML	3.5	6.7	7.6	11
9	38.424	-13.586	15	ML	3.0	4.4	7.4	17
			75	DCM	8.0	5.5	12.8	23
11	40.528	-13.191	15	ML	8.4	8.2	14.1	17
13	42.337	-12.884	15	ML	6.9	3.0	12.7	43
			47	DCM	16.0	12.2	21.3	18
15	44.283	-12.605	15	ML	5.8	9.0	16.5	18
			60	DCM	15.8	9.9	14.7	15
16	45.917	-12.363	10	ML	14.2	17.2	35.1	20
18	47.569	-12.110	25	ML	8.8	10.6	27.6	26
19	49.382	-11.829	15	ML	n.d.	5.7	31.1	55
19	49.382	-11.829	30	ML	n.d.	5.5	14.9	27
21	51.000	-11.567	15	ML	8.6	8.4	25.5	30
25	58.002	-16.516	10	ML	7.5	18.7	23.5	13
27	59.499	-18.067	20	ML	9.7	15.7	25.5	16
29	60.684	-19.339	10	ML	6.6	12.9	16.5	13
30	61.715	-20.489	15	ML	n.d.	28.1	28.4	10
32	62.800	-21.736	10	ML	11.7	31.9	3.9	7

Within the DCM in the oligotrophic southern region, PA, VA and HNF abundances were higher compared to the upper ML, with 8.6±2.1 $x10^8$ prokaryotes l^{-1}, 13±0.4 $x10^9$ viruses l^{-1} and 6.5±2.3 $x10^5$ HNF l^{-1} (Fig. 2). As for the ML, VA in the DCM was also positively correlated to PA. PA and VA were positively associated with the $Z_{eu}PO_4$ and negatively with NH_4^+ (Table S6). VPR in the DCM was similar to the ratios in the ML (2-sample *t* test; $\alpha = 0.05$, $p = 0.17$). However, VPR in the DCM was positively related to N^2 and inversely related to $Z_{eu}NO_3$ and N:P (Table S6). HNF abundance was not found to have a significant correlation to any of the environmental or biological parameters measured (Table S5 and S6).

Heterotrophic prokaryotic production

In the ML, PP_L averaged 1.0±0.4 $x10^8$ cells l^{-1} d^{-1} or 1.3 ± 0.5 µgC l^{-1} d^{-1} south of 45°N (Stn 3 - 15) and increased 2-fold (2.4±1.4 $x10^8$ cells l^{-1} d^{-1}) in the north (Table

S1). PP_L varied significantly with latitude and was positively associated with PO_4^{3-} concentrations (Table S5). PP_{gross} in the ML averaged 5.8±2.0 x 10^8 cells l^{-1} d^{-1} (or 7.2 µg C l^{-1} d^{-1}) for the southern stations and was 1.4-fold higher in the northern region (8.4±4.8 x 10^8 cells l^{-1} d^{-1} or 10.4±6.0 µg C l^{-1} d^{-1}) (Table S1). PP_{gross} was significantly correlated to N:P (Table S5). In the DCM, PP_L and PP_{gross} were not significantly different from the surface waters of the same region and were on average 1.3±0.6 x10^8 and 8.4±5.0 x10^8 cells l^{-1} d^{-1}, respectively (Table S1). Within this layer, PP_L and PP_{gross} were significantly correlated to PA, $Z_{eu}PO_4$ and to each other, and negatively to NH_4^+ (Table S6).

Prokaryotic mortality

Lytic VP in the ML increased from 0.6±0.4 x10^{10} viruses l^{-1} d^{-1} in the oligotrophic south to 1.4±1.7 x10^{10} viruses l^{-1} d^{-1} in the north, corresponding to a greater than 2-fold increase in VMM from 3.2±1.9 to 7.0±8.7 x10^8 cell lysed l^{-1} d^{-1} (Fig. 3A, Table 3). Lytic VP was positively correlated to PP_{gross} and N:P (Table S5). Mitomycin C inducible prophages were only detected in a few ML samples (i.e., Stn 11, 15, 19 and 25) and rates varied from 0.1 to 1.0 x10^{10} viruses l^{-1} d^{-1} (Fig. 3B). The prophage induction in the ML was, nonetheless, significantly correlated to $Z_{eu}NO_3$ (Table S5). On average, PPM in the ML increased 1.6-fold between the southern oligotrophic region (2.2±1.0 x10^8) and the north (3.6±3.5 x10^8 cells l^{-1} d^{-1}) (Table 3), which was largely due to differences in PA (Fig. 2A) and not the actual HNF grazing rates (i.e., 0.4±0.2 d^{-1} in the south to 0.3±0.2 d^{-1} in the north; Fig. 3C). The HNF grazing rate in the ML was positively correlated to temperature and inversely to latitude, PP_L and VA (with PP_L and VA positively related to latitude; Table S5).

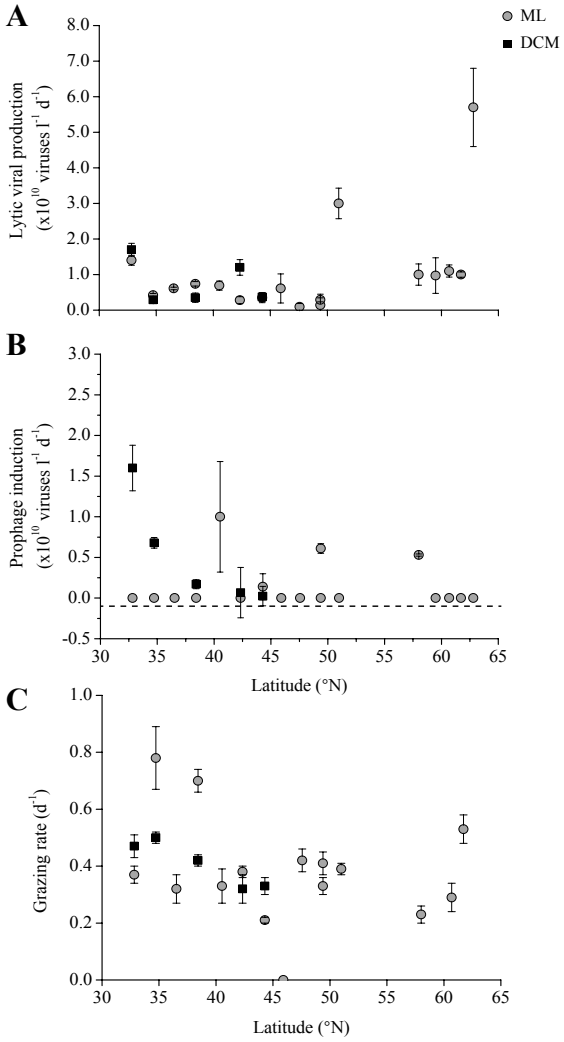

Figure 3. Average mortality rates of prokaryotes by (**A**) lytic viral production, (**B**) inducible prophages and (**C**) grazing measured over the Northeast Atlantic during the STRATIPHYT cruise. Error bars represent standard error (N = 3).

Lytic VP and VMM did not significantly vary between the ML and DCM of oligotrophic regions, i.e., 0.8±0.6 x10^{10} viruses l^{-1} d^{-1} and VMM of 3.8±3.1 x10^{8} cells lysed l^{-1} d^{-1}, respectively (Fig. 3A, Table 3). In the DCM, lytic VP was not only correlated to PP_{gross} but also to PP_{L}, PA, and VA. Inducible prophages were detected within all DCM samples and were found to be significantly related to latitude and Chl *a*, whereby the rates declined hyperbolically from 16.0 to 0.2 x10^{9} viruses l^{-1} d^{-1} with

increasing latitude and Chl *a* concentrations (Fig. 3B, Table S6). HNF grazing rates in the DCM (average of 0.4±0.1 d^{-1}) were also comparable to rates in the ML, however the resulting PMM in the DCM (3.1±0.8 x10^8 cell l^{-1} d^{-1}) were higher (comparable to the ML losses in the north; Table 3). HNF grazing rates in the DCM were inversely correlated to lytic VP, VA and PA, whereby PA was directly linked to VA. PPM was positively tied to VPR and N^2 (and factors associated to these 2 factors; Table S6).

Table 3. Prokaryotic standing stock (SS; µg l^{-1}), production (PP_{gross}) and loss rates (virus mediated, VMM, and grazing mediated, PMM, mortality) in organic carbon (µg l^{-1} d^{-1}) and in terms of percentage of total available carbon (TAC_{max}; determined as the sum of SS and PP_{gross}). Total mortality is abbreviated as TM. n.d. = not determined.

Station	Depth Layer	SS	PP_{gross}	VMM	PMM	TM:PP_{gross}	TAC_{max}	% TAC_{lysed}	% TAC_{grazed}
3	ML	9.0	11.2	8.6	2.8	1.0	20.1	42.5	13.7
	DCM	13.9	16.6	10.4	5.2	0.9	30.6	34.0	17.0
5	ML	9.6	7.1	2.6	5.2	1.1	16.6	15.5	31.1
	DCM	9.7	5.6	1.8	3.8	1.0	15.3	11.9	24.9
7	ML	8.3	n.d.	3.8	2.3	n.d.	n.d.	n.d.	n.d.
9	ML	5.4	7.6	4.6	2.7	1.0	13.0	35.1	21.0
	DCM	6.8	4.6	2.1	2.4	1.0	11.4	18.8	20.5
11	ML	10.2	7.6	4.2	2.8	0.9	17.8	23.9	15.9
13	ML	3.7	4.2	1.7	1.2	0.7	7.9	22.1	14.8
	DCM	15.1	12.0	7.2	4.2	1.0	27.1	26.6	15.3
15	ML	11.2	5.5	2.2	2.1	0.8	16.7	13.0	12.5
	DCM	12.2	6.1	2.3	3.4	0.9	18.3	12.5	18.7
16	ML	21.4	7.1	3.8	0.0	0.5	28.5	13.3	0.0
18	ML	13.2	6.8	0.6	4.5	0.8	20.0	2.9	22.6
19	ML	7.0	3.9	0.9	2.4	0.8	10.9	8.0	21.7
19	ML	6.8	4.7	1.8	1.9	0.8	11.5	15.7	16.8
21	ML	10.4	21.5	18.7	3.3	1.0	31.9	58.6	10.5
25	ML	23.2	13.5	6.5	4.7	0.8	36.7	17.6	12.8
27	ML	19.4	11.3	6.0	n.d.	n.d.	30.8	19.6	0.0
29	ML	15.9	14.4	7.1	4.0	0.8	30.3	23.2	13.1
30	ML	34.8	n.d.	6.5	14.4	n.d.	n.d.	n.d.	n.d.
32	ML	39.5	n.d.	35.5	n.d.	n.d.	n.d.	n.d.	n.d.

Averaged overall, PMM was nearly 2-fold lower at 2.8 x10^8 cells l^{-1} d^{-1} compared to that of VMM at 5.2 x10^8 cells l^{-1} d^{-1} (Table 3). Comparing mortality factors as a function of latitude revealed that VMM was, in most cases, the dominant regulating factor (Fig. 4). Total mortality (TM) (viral lysis plus grazing) ranged from 0.2 to 2.9 x10^9 cells l^{-1} d^{-1}, and was on average slightly lower than PP_{gross} (i.e, average TM:PP_{gross} of ~0.9; Fig. 5A). However, the discrepancy between TM and

PP_{gross} increased significantly with latitude in the ML (Fig. 5B; Table S5), indicating net heterotrophic production in the surface waters at higher latitudes.

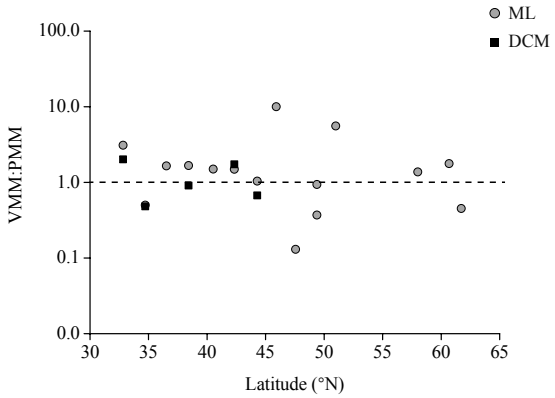

Figure 4. The contribution of viral lysis to prokaryote mortality. Ratio of viral-mediated mortality (VMM) to protist-mediated mortality (PMM) as function of latitude. Rates were determined using FLP and virus reduction experiments performed during the STRATIPHYT cruise. Dotted line indicates a 1:1 relationship of viral lysis to grazing.

TAC in the ML ranged from a minimum of 5 - 27 (TAC_{min}) to a maximum of 8 - 37 μg C l^{-1} d^{-1} (TAC_{max}). On average TAC_{max} was 1.5 times higher than TAC_{min}. TAC_{max} increased 1.6-fold between the oligotrophic south and the north, corresponding to average values increasing from 15.3±4.3 to 25.1±9.7 μg C l^{-1}. TAC concentrations in the DCM of oligotrophic stations were slightly higher with TAC_{max} of 20.6±8.1 μg C l^{-1} (Table 3). The percentage of TAC_{min} lost (i.e., viral lysis plus grazing), sometimes exceeded 100% (up to 203%), which is due to the lack of consideration of production which can be grazed and lysed during measurement. Therefore, the usage of TAC_{min} can lead to unrealistic losses in total available carbon. Using TAC_{max}, the percentage lost ranged from 13 - 69% with an average of 39%. The percentage of TAC_{max} lysed was highest in the ML of the southern oligotrophic region, i.e., 25±11 as compared to 20±17% in the north. In contrast, TAC_{max} grazed in the ML decreased from 18±7 in south to 12±9 in the north. TAC_{max} lysed and grazed in the DCM were comparable to the ML of the same region, i.e., 21±10 and 19±4 %.

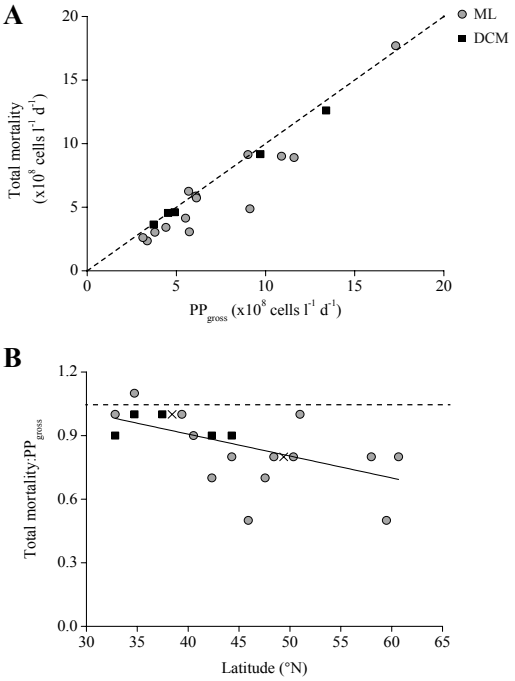

Figure 5. The relationship between total mortality and gross growth of heterotrophic prokaryotes measured over the Northeast Atlantic during the STRATIPHYT cruise. (**A**) Relationship between the total mortality (grazing + viral lysis) and PP_{gross} (in cells l^{-1} d^{-1}), and (**B**) Ratio of total mortality to PP_{gross} of heterotrophic prokaryotes as function of latitude. Dotted lines indicate a 1:1 relationship, and the solid line is a linear regression through the data. Crosses mark the center of overlapping points which are then plotted on either side of the mark..

Discussion

The strong positive correlation between VA and PA has been reported previously for the North Atlantic Ocean and confers with evidence that the majority of viruses in the ocean infect the numerically dominant prokaryotic hosts (Suttle 2007). Viruses are dependent on their host to provide the necessary energy, resources and machinery required for viral replication. Consequently, factors regulating the abundance and physiology of their hosts, as well as their production and removal are also important in governing virus dynamics (Mojica and Brussaard 2014). VA was positively correlated with PP_L, suggesting that host physiology and generation time may have been important factor regulating virus abundance during our study period (Proctor et al. 1993; Moebus 1996; Middelboe 2000). In fact, lytic VP in both the ML and DCM were significantly correlated to heterotrophic prokaryotic

production. Furthermore, lytic VP in the ML was positively correlated to N:P which may suggest that the availability of the inorganic nutrients affected viral production, most likely via nutrient-limited host physiology (Moebus 1996; Motegi and Nagata 2007).

Indeed, heterotrophic prokaryotic production was uncoupled from phytoplankton biomass (Chl *a*) and instead linked to nutrient availability (i.e., PP_L to PO_4^{3-} and PP_{gross} to N:P). Several studies indicated that in oligotrophic regions of the North Atlantic Ocean heterotrophic prokaryotes can be limited by the availability of inorganic nutrients (Cotner et al. 1997; Rivkin and Anderson 1997; Mills et al. 2008). The dominance and relatively high abundance (up to 2 $x10^8$ cells l^{-1}) of pico-sized phytoplankton present during our study period (Mojica et al. 2015) could have efficiently competed for inorganic nutrients and thereby increased the potential for limitation. Alternatively, the nutrient limitation of phytoplankton can affect both the quantity and quality of DOM released, and thus the efficiency with which it can be utilized (Obernosterer and Herndl 1995; Gardes et al. 2012). In the marine environment, trends in prevalence of lysogeny across different systems suggests that it may represent a survival strategy to endure conditions of low host productivity and abundance (Williamson et al. 2002; Weinbauer et al. 2003; Payet and Suttle 2013). We found no direct correlation between lysogeny, inorganic nutrient concentrations, PA or heterotrophic prokaryotic production. However, correlations presented here were to total community abundance and production, and thus correlations may be obscured if induction sensitive host-phage systems were not dominant members of the prokaryotic community. Inducible prophages were only detected at 4 stations within the ML of our study period, with a positive correlation to $Z_{eu}NO_3$. The reason for this connection remains unclear due the lack of association in the ML between $Z_{eu}NO_3$ and other variables measured. An alternative explanation for the lack of inducible prophages in the surface ML may be prolonged exposure to high levels of solar radiation (particularly UV), which can induce lysogens and result in a reduced phophage yield from Mitomycin C addition (Wilcox and Fuhrman 1994; Weinbauer and Suttle 1999). In contrast, inducible prophages were detected within the DCM of every southern station tested and was negatively correlated to Chl *a* (this study). Chl *a* is an indication of phytoplankton biomass but is not necessarily indicative of numerical abundance (as small phytoplankton contribute relatively less to biomass compared to larger phytoplankton). Pico-sized *Prochlorococcus* spp. were dominant in the DCM (93%), with abundances decreasing with latitude (Mojica et al. 2015). Consequently,

competition for inorganic nutrients between autotrophic and heterotrophic prokaryotes may have pushed nutrient limitation to a point at which lytic viral production could no longer be effectively sustained and consequently triggered a switch to lysogenic infection. This hypothesis is supported by evidence that inorganic nutrients may at times be an important factor modulating lysogeny in natural heterotrophic populations (Williamson et al. 2002; Motegi and Nagata 2007). However, further research is required to better understand the role that inorganic nutrient availability plays in regulating viral life strategy selection in natural heteroptrophic prokaryotic host populations.

In general, heterotrophic production, abundances and mortality in the ML was higher for the northern region than the south. However, PMM did not increase uniformly with PP_L and VMM, implying that grazing pressure was reduced in the north. Indeed, correlation analysis showed a significant inverse relationship between HNF grazing rates and latitude and a positive correlation to temperature. This supports evidence that warming will increase bacterial losses due to protist grazing (Sarmento et al. 2010). Alternatively top-down control of protists may have been higher in the northern region (Rychert et al. 2014). Strong top-down control of bacterivores could also explain the lack of correlation between HNF and other measured parameters. Accordingly, predation of protist would relax competition between HNF and viruses for bacterial prey, which would account for the negative correlations of HNF grazing rate with VA, and PMM with VBR. This suggests that viral-induced mortality may also have played a regulatory role by controlling prokaryotic prey density and/or by infecting HNF (Garza and Suttle 1995; Nagasaki et al. 1995; Massana et al. 2007). More research is needed specifically studying the different forcing factors for HNF distribution and activity before decisive conclusions can be drawn. In any case, the lower grazing losses in the northern region do clarify the lack of correlation found between PP_L and PP_{gross} in the ML. Following the hypothesis for a regulatory role of viral-induced mortality in controlling prokaryotic prey density (as indicated through the inverse correlation of HNF grazing with VA and lytic VP), would also explain the higher PA in the DCM despite comparable PP_L between the DCM and the ML. The counter argument that organic resources in the DCM are limited is argued against by the higher phytoplankton abundance and Chl *a* concentration in the DCM compared to the ML.

Contribution to total mortality and consequences for carbon cycling

Overall, VMM was the dominant loss factor regulating prokaryotic populations in the surface waters of the Northeast Atlantic Ocean along a latitudinal gradient in stratification during the summer of 2009. Averaged over all stations and depths, 25% of the TAC was cycled back into the water column by viral activity compared to 14% entering the food web by grazing, emphasizing the role of viruses as important drivers for carbon cycling in the Northeast Atlantic. Moreover, VMM and PMM varied with trophic status, i.e., both were higher in the north compared to the oligotrophic southern region (2.1 and 1.6-fold, respectively). However, the ratio of TM to PP_{gross} decreased over the latitudinal gradient (due to the reduced grazing pressure in the north), thereby representing a gradual change from a system regulated by high turnover in regions of strong stratification to net heterotrophic production with reduced stratification.

Several studies predict that global warming will result in stronger temperature stratification in the North Atlantic Ocean (Sarmiento 2004; Polovina et al. 2008) and thus reduce total availability of photosynthetic carbon at higher latitudes. Our results indicate that in summer this may also lead to a reduction in heterotrophic prokaryote production at these higher latitudes, i.e., as the system moves away from net heterotrophic production towards a steady-state situation where production is balanced by loss. The relative contributions of the different pathways (i.e., grazing versus viral lysis) is likely to remain consistent, with viral lysis cycling more of the organic carbon back into the water column than is being transferred to higher trophic levels by grazers.

Acknowledgements

The STRATIPHYT project was supported by the division for Earth and Life Sciences Foundation (ALW), with financial aid from the Netherlands Organization for Scientific Research (NWO) (Grant number 839.08.420). We thank the captains and shipboard crews of R/V Pelagia and scientific crews during the cruises, with special thanks to Tea de Vries. We acknowledge the support of NIOZ-Marine Research Facilities (MRF) on-shore and on-board.

Reference

Angly FE, Felts B, Breitbart M, Salamon P, Edwards RA, Carlson C, Chan AM, Haynes M, Kelley S, Liu H, Mahaffy JM, Mueller JE, Nulton J, Olson R, Parsons R, Rayhawk S, Suttle CA, Rohwer F (2006) The marine viromes of four oceanic regions. PLOS Biology 4: e368. doi: 10.1371/journal.pbio.0040368

Behrenfeld MJ, O 'Malley RT, Siegel DA, McClain CR, Sarmiento JL, Feldman GC, Milligan AJ, Falkowski PG, Letelier RM, Boss ES (2006) Climate-driven trends in contemporary ocean productivity. Nature 444:752-755

Bray NA, Fofonoff NP (1981) Available potential energy for mode eddies. Journal of Physical Oceanography 11:30-47

Brussaard CPD, Wilhelm SW, Thingstad TF, Weinbauer MG, Bratbak G, Heldal M, Kimmance SA, Middelboe M, Nagasaki K, Paul JH, Schroeder DC, Suttle CA, Vaque D, Wommack KE (2008) Global-scale processes with a nanoscale drive: the role of marine viruses. The ISME Journal 2:575-578

Campbell BJ, Waidner LA, Cottrell MT, Kirchman DL (2008) Abundant proteorhodopsin genes in the North Atlantic Ocean. Environmental Microbiology 10:99-109

Carlson CA, Ducklow HW (1996) Growth of bacterioplankton and consumption of dissolved organic carbon in the Sargasso Sea. Aquatic Microbial Ecology 10:69-85

Chibani-Chennoufi S, Bruttin A, Dillmann ML, Brussow H (2004) Phage-host interaction: an ecological perspective. Journal of Bacteriology 186:3677-3686

Church MJ, Hutchins DA, Ducklow HW (2000) Limitation of bacterial growth by dissolved organic matter and iron in the Southern Ocean. Applied and Environmental Microbiology 66:455-466

Cotner JB, Ammerman JW, Peele ER, Bentzen E (1997) Phosphorus-limited bacterioplankton growth in the Sargasso Sea. Aquatic Microbial Ecology 13:141-149

Fenchel T, Finlay BJ (1983) Respiration rates in heterotrophic, free-living protozoa. Microbial Ecology 9:99-122

Fuhrman JA (1999) Marine viruses and their biogeochemical and ecological effects. Nature 399:541-548

Fukuda R, Ogawa H, Nagata T, Koike I (1998) Direct determination of carbon and nitrogen contents of natural bacterial assemblages in marine environments. Applied and Environmental Microbiology 64:3352-3358

Furrer R, Nychka D, Sain S (2012) fields: Tools for spatial data. R package version 6.7

Gama JA, Reis AM, Domingues I, Mendes-Soares H, Matos AM, Dionisio F (2013) Temperate bacterial viruses as double-edged swords in bacterial warfare. PLOS One 8:e59043. doi: 10.1371/journal.pone.0059043

Gardes A, Ramaye Y, Grossart HP, Passow U, Ullrich MS (2012) Effects of *Marinobacter adhaerens* HP15 on polymer exudation by *Thalassiosira weissflogii* at different N:P ratios. Marine Ecology Progress Series 461:1-14

Garza DR, Suttle CA (1995) Large double-stranded DNA viruses which cause the lysis of a marine heterotrophic nanoflagellate (*Bodo* sp) occur in natural marine viral communities. Aquatic Microbial Ecology 9:203-210

Gasol JM, Vazquez-Dominguez E, Vaque D, Agusti S, Duarte CM (2009) Bacterial activity and diffusive nutrient supply in the oligotrophic Central Atlantic Ocean. Aquatic Microbial Ecology 56:1-12

Gobler CJ, Hutchins DA, Fisher NS, Cosper EM, Sanudo-Wilhelmy SA (1997) Release and bioavailability of C, N, P, Se, and Fe following viral lysis of a marine chrysophyte. Limnology and Oceanography 42:1492-1504

Gomez-Consarnau L, Akram N, Lindell K, Pedersen A, Neutze R, Milton DL, Gonzalez JM, Pinhassi J (2010) Proteorhodopsin phototrophy promotes survival of marine bacteria during starvation. PLOS Biology 8: E1000358. doi: 10.1371/journal.pbio.1000358

Grasshoff K (1983) Determination of nitrate. In: Grasshoff K, Erhardt M, Kremeling K (eds) Methods of Seawater Analysis. Verlag Chemie, Weinheim, Germany

Helder W, de Vries RTP (1979) An automatic phenol-hypochlorite method for the determination of ammonia in sea and brackish water. Netherlands Journal of Sea Research 13:154-160

Hoegh-Guldberg O, Bruno JF (2010) The impact of climate change on the world's marine ecosystems. Science 328:1523-1528

Huisman J, Thi NNP, Karl DM, Sommeijer B (2006) Reduced mixing generates oscillations and chaos in the oceanic deep chlorophyll maximum. Nature 439:322-325

Jurado E, Dijkstra HA, van der Woerd HJ (2012a) Microstructure observations during the spring 2011 STRATIPHYT-II cruise in the northeast Atlantic. Ocean Science 8:945-957

Jurado E, van der Woerd HJ, Dijkstra HA (2012) Microstructure measurements along a quasi-meridional transect in the northeastern Atlantic Ocean. Journal of Geophysical Research 117: C04016. doi: 10.1029/2011JC007137

Kirchman D (2001) Measuring bacterial biomass production and growth rates from leucine incorporation in natural aquatic environments. In: Paul JH (ed) Methods in Microbiology, vol. 30. Academic Press, San Diego

Kirchman DL (1990) Limitation of bacterial growth by dissolved organic matter in the subarctic Pacific. Marine Ecology Progress Series 62:47-54

Koroleff F (1969) Direct determination of ammonia in natural waters as indophenol blue. Coun. Meet. int. Coun. Explor. Sea **C.M.-ICES/C:** 9

Marie D, Brussaard CPD, Thyrhaug R, Bratbak G, Vaulot D (1999) Enumeration of marine viruses in culture and natural samples by flow cytometry. Applied and Environmental Microbiology 65:45-52

Massana R, del Campo J, Dinter C, Sommaruga R (2007) Crash of a population of the marine heterotrophic flagellate *Cafeteria roenbergensis* by viral infection. Environmental Microbiology 9:2660-2669

Michelou VK, Cottrell MT, Kirchman DL (2007) Light-stimulated bacterial production and amino acid assimilation by cyanobacteria and other microbes in the North Atlantic Ocean. Applied and Environmental Microbiology 73:5539-5546

Middelboe M (2000) Bacterial growth rate and marine virus-host dynamics. Microbial Ecology 40:114-124

Middelboe M, Jørgensen NOG (2006) Viral lysis of bacteria: an important source of dissolved amino acids and cell wall compounds. Journal of the Marine Biological Association of the United Kingdom 86:605-612

Middelboe M, Jørgensen NOG, Kroer N (1996) Effects of viruses on nutrient turnover and growth efficiency of noninfected marine bacterioplankton. Applied and Environmental Microbiology 62:1991-1997

Mills MM, Moore CM, Langlois R, Milne A, Achterberg E, Nachtigall K, Lochte K, Geider RJ, La Roche J (2008) Nitrogen and phosphorus co-limitation of bacterial productivity and growth in the oligotrophic subtropical North Atlantic. Limnology and Oceanography 53:824-834

Moebus K (1996) Marine bacteriophage reproduction under nutrient-limited growth of host bacteria. I. Investigations with six phage-host systems. Marine Ecology Progress Series 144:1-12

Mojica KDA, Brussaard CPD (2014) Factors affecting virus dynamics and microbial host-virus interactions in marine environments. FEMS Microbiology Ecology 89:495-515

Mojica KDA, Evans C, Brussaard CPD (2014) Flow cytometric enumeration of marine viral populations at low abundances. Aquatic Microbial Ecology 71:203-209

Mojica KDA, van de Poll WH, Kehoe M, Huisman J, Timmermans KR, Buma AGJ, van der Woerd HJ, Hahn-Woernle L, Dijkstra HA, Brussaard CPD (2015). Phytoplankton community structure in relation to vertical stratification along a north-south gradient in the Northeast Atlantic Ocean. Limnology and Oceanography (*in press*). doi: 10.1002/lno.10113

Motegi C, Nagata T (2007) Enhancement of viral production by addition of nitrogen or nitrogen plus carbon in subtropical surface waters of the South Pacific. Aquatic Microbial Ecology 48:27-34

Murphy J, Riley JP (1962) A modified single solution method for the determination of phosphate in natural waters. Analytica Chimica Acta 27:31-36

Nagasaki K, Ando M, Imai I, Itakura S, Ishida Y (1995) Virus-like particles in unicellular apochlorotic microorganisms in the coastal water of Japan. Fisheries Science 61:235-239

Obernosterer I, Herndl GJ (1995) Phytoplankton extracellular release and bacterial growth: dependence on the inorganic N:P Ratio. Marine Ecology Progress Series 116:247-257

Parada V, Herndl GJ, Weinbauer MG (2006) Viral burst size of heterotrophic prokaryotes in aquatic systems. Journal of the Marine Biological Association of the United Kingdom 86:613-621

Paul JH, Weinbauer M (2010) Detection of lysogeny in marine environments. In: Wilhelm SW, Weinbauer M, Suttle CA (eds) Manual of Aquatic Viral Ecology. ASLO

Payet JP, Suttle CA (2013) To kill or not to kill: the balance between lytic and lysogenic viral infection is driven by trophic status. Limnology and Oceanography 58:465-474

Polovina JJ, Howell EA, Abecassis M (2008) Ocean's least productive waters are expanding. Geophysical Research Letters 35: L03618. doi: 10.1029/2007GL031745

Proctor LM, Okubo A, Fuhrman JA (1993) Calibrating estimates of phage-induced mortality in marine bacteria: ultrastructural studies of marine bacteriophage development from one-step growth experiments. Microbial Ecology 25:161-182

R Development Core Team (2012) R: A language and environment for statistical computing. R Foundation for Statistical Computing: Vienna, Austria, ISBN 3-900051-07-0, http://www.R-project.org

Revelle W (2014) psych: Procedures for Psychological, Psychometric, and Personality Research.

Rivkin RB, Anderson MR (1997) Inorganic nutrient limitation of oceanic bacterioplankton. Limnology and Oceanography 42:730-740

Rychert K, Nawacka B, Majchrowski R, Zapadka T (2014) Latitudinal pattern of abundance and composition of ciliate communities in the surface waters of the Atlantic Ocean. Oceanological and Hydrobiological Studies 43:436-441

Sabine CL, Feely RA, Gruber N, Key RM, Lee K, Bullister JL, Wanninkhof R, Wong CS, Wallace DWR, Tilbrook B, Millero FJ, Peng TH, Kozyr A, Ono T, Rios AF (2004) The oceanic sink for anthropogenic CO_2. Science 305:367-371

Sarmento H, Montoya JM, Vazquez-Dominguez E, Vaque D, Gasol JM (2010) Warming effects on marine microbial food web processes: how far can we go when it comes to predictions? Philosophical Transactions of the Royal Scociety B 365:2137-2149

Sarmiento JL (2004) Response of ocean ecosystems to climate warming. Global Biogeochemical Cycles 18: GB3003. doi: 10.1029/2003GB002134

Schlitzer R (2002) Interactive analysis and visualization of geoscience data with Ocean Data View. Computers and Geoscience 28:1211-1218

Sheik AR, Brussaard CPD, Lavik G, Lam P, Musat N, Krupke A, Littmann S, Strous M, Kuypers MMM (2014) Responses of the coastal bacterial community to viral infection of the algae *Phaeocystis globosa*. The ISME Journal 8:212-225

Sherr BF, Sherr EB, Fallon RD (1987) Use of monodispersed, fluorescently labeled bacteria to estimate *In situ* protozoan bacterivory. Applied and Environmental Microbiology 53:958-965

Simon M, Azam F (1989) Protein content and protein synthesis rates of planktonic marine bacteria. Marine Ecology Progress Series 51:201-213

Straile D (1997) Gross growth efficiencies of protozoan and metazoan zooplankton and their dependence on food concentration, predator-prey weight ratio, and taxonomic group. Limnology and Oceanography 42:1375-1385

Suttle CA (2005) Viruses in the sea. Nature 437:356-361

Suttle CA (2007) Marine viruses - major players in the global ecosystem. Nature Reviews 5:801-812

Talley L, Pickard G, Emery W, Swift J (2011) Typical distribution of water characteristics. Descriptive Physical Oceanography. Elsevier Ltd., London

van de Poll WH, Kulk G, Timmermans KR, Brussaard CPD, van der Woerd HJ, Kehoe MJ, Mojica KDA, Visser RJW, Rozeman PD, Buma AGJ (2013) Phytoplankton chlorophyll *a* biomass, composition, and productivity along a temperature and stratification gradient in the northeast Atlantic Ocean. Biogeosciences 10:4227-4240

Vaulot D (1989) CYTOPC: Processing software for flow cytometric data. Signal and Noise 2:8

Weinbauer MG (2004) Ecology of prokaryotic viruses. FEMS Microbiology Reviews 28:127-181

Weinbauer MG, Brettar I, Hofle MG (2003) Lysogeny and virus-induced mortality of bacterioplankton in surface, deep, and anoxic marine waters. Limnology and Oceanography 48:1457-1465

Weinbauer MG, Suttle CA (1999) Lysogeny and prophage induction in coastal and offshore bacterial communities. Aquatic Microbial Ecology 18:217-225

Wilcox RM, Fuhrman JA (1994) Bacterial viruses in coastal seawater: lytic rather than lysogenic production. Marine Ecology Progress Series 114:35-45

Wilhelm SW, Brigden SM, Suttle CA (2002) A dilution technique for the direct measurement of viral production: a comparison in stratified and tidally mixed coastal waters. Microbial Ecology 43:168-173

Wilhelm SW, Suttle CA (1999) Viruses and nutrient cycles in the sea - viruses play critical roles in the structure and function of aquatic food webs. Bioscience 49:781-788

Williamson SJ, Houchin LA, McDaniel L, Paul JH (2002) Seasonal variation in lysogeny as depicted by prophage induction in Tampa Bay, Florida. Applied and Environmental Microbiology 68:4307-4314

Winget DM, Williamson KE, Helton RR, Wommack KE (2005a) Tangential flow diafiltration: an improved technique for estimation of virioplankton production. Aquatic Microbial Ecology 41:221-232

Supporting information

Table S1. Prokaryotic production (PP) determined by leucine incorporation (PP_L) and net production from whole water incubations (PPnet) with rates of viral mediated mortality (VMM) and protist mediated mortality (PMM). PP_{gross} is PP_L corrected for losses (assuming a 30% growth efficiency for grazing). All units are in $x10^8$ cells l^{-1} d^{-1}. n.d. = not determined.

Station	Depth Layer	PP_L	PP_{net}	VMM	PMM	PP_{gross}
3	ML	0.6	0.1	6.9	2.2	9.0
	DCM	2.1	0.2	8.4	4.2	13.4
5	ML	0.7	5.4	2.1	4.2	5.7
	DCM	0.9	0.1	1.5	3.1	4.5
7	ML	n.d.	5.4	3.1	1.9	n.d.
9	ML	0.9	0.3	3.7	2.2	6.1
	DCM	0.7	2.6	1.7	1.9	3.7
11	ML	1.1	1.3	3.4	2.3	6.1
13	ML	1.3	2.0	1.4	0.9	3.4
	DCM	1.5	1.2	5.8	3.4	9.7
15	ML	1.5	5.3	1.7	1.7	4.4
	DCM	1.1	0.8	1.8	2.8	4.9
16	ML	2.7	2.5	3.1	0.0	5.7
18	ML	2.5	4.8	0.5	3.7	5.5
19	ML	1.1	9.4	0.7	1.9	3.1
19	ML	1.2	4.8	1.5	1.6	3.8
21	ML	0.4	1.0	15.0	2.7	17.3
25	ML	3.0	7.8	5.2	3.8	10.9
27	ML	4.3	0.2	4.9	n.d.	9.1
29	ML	3.7	2.1	5.7	3.2	11.6
30	ML	n.d.	4.5	5.2	11.6	n.d.
32	ML	n.d.	0.6	28.7	n.d.	n.d.

Table S2. Brunt-Väisälä frequency (N^2), vertical mixing coefficient (K_T) and nutrient flux of PO_4^{3-} and NO_3^- at the depth of the euphotic zone for water sampled in the North Atlantic for heterotrophic prokaryotic production, viral production and grazing experiments. Abbreviations for depth layer are mixed layer (ML) and deep chlorophyll maximum (DCM). NA indicates that data were not available.

Station	Latitude (°N)	Longitude (°E)	Depth (m)	Depth Layer	N^2 ($x10^{-5}$ rad^2 s^{-1})	$LogK_T$ (m^{-2} s^{-1})	$Z_{eu}PO_4$ (mmol m^{-2} d^{-1})	$Z_{eu}NO_3$ (mmol m^{-2} d^{-1})
3	32.825	-14.589	15	ML	NA	-1.8	-0.013	-0.013
			60	DCM	NA	-4.7		
5	34.720	-14.258	15	ML	4.7	-2.5	-0.003	0.148
			85	DCM	14.2	-5.0		
7	36.526	-13.934	15	ML	6.6	-3.4	0.012	0.017
9	38.424	-13.586	15	ML	3.2	-3.2	0.002	0.011
			75	DCM	NA	-5.1		
11	40.528	-13.191	15	ML	2.5	-3.1	0.008	0.011
13	42.337	-12.884	15	ML	1.1	-3.0	0.003	0.018
			47	DCM	22.0	-4.8		
15	44.283	-12.605	15	ML	4.8	-2.6	-0.025	-0.149
			60	DCM	12.9	-4.7		
16	45.917	-12.363	10	ML	NA	-2.7	0.064	0.890
18	47.569	-12.110	25	ML	NA	-3.1	0.068	0.755
19	49.382	-11.829	15	ML	4.8	-2.6	0.003	0.401
19	49.382	-11.829	30	ML	2.5	-3.7	0.003	0.401
21	51.000	-11.567	15	ML	NA	-2.5	0.090	1.217
25	58.002	-16.516	10	ML	NA	-2.8	0.208	4.094
27	59.499	-18.067	20	ML	4.0	-3.8	0.064	0.487
29	60.684	-19.339	10	ML	4.4	-2.8	2.015	34.966
30	61.715	-20.489	15	ML	NA	-3.3	0.159	1.163
32	62.800	-21.736	10	ML	2.1	-4.1	0.024	0.199

Table S3. Spearman rank correlation coefficients (above the diagonal) and p-values (below the diagonal) of physicochemical paramters and Chl *a* for the ML samples. Abbreviations are for latitude (Lat), temperature (Temp), vertical mixing coefficient (K_T), Brunt-Väisälä frequency (N^2) and nutrient flux into the euphotic zone (Z_{eu}*). n.s. indicates non-significance at $\alpha = 0.05$.

	Lat	Temp	Salinity	K_T	N^2	$Z_{eu}PO_4$	$Z_{eu}NO_3$	PO_4^{3-}	NH_4^+	NO_2^-	NO_3^-	N:P	Chl *a*
Lat		-1.00	-0.94	n.s.	n.s.	n.s.	n.s.	0.89	n.s.	n.s.	0.84	n.s.	n.s.
Temp	0.00		0.94	n.s.	n.s.	n.s.	n.s.	-0.89	n.s.	n.s.	-0.84	n.s.	n.s.
Salinity	0.00	0.00		n.s.	n.s.	n.s.	n.s.	-0.94	n.s.	n.s.	-0.90	n.s.	n.s.
K_T	1.00	1.00	1.00		n.s.	n.s.	n.s.	n.s.	n.s.	n.s.	n.s.	n.s.	n.s.
N^2	1.00	1.00	1.00	0.09		n.s.	n.s.	n.s.	n.s.	n.s.	n.s.	n.s.	n.s.
$Z_{eu}PO_4$	1.00	1.00	1.00	1.00	1.00		n.s.	n.s.	-0.94	-0.99	n.s.	-0.83	-1.00
$Z_{eu}NO_3$	1.00	1.00	1.00	1.00	1.00	1.00		n.s.	n.s.	n.s.	n.s.	n.s.	n.s.
PO_4^{3-}	0.00	0.00	0.00	1.00	1.00	1.00	1.00		n.s.	n.s.	0.99	n.s.	n.s.
NH_4^+	1.00	1.00	1.00	1.00	1.00	0.00	1.00	1.00		0.89	n.s.	0.94	0.94
NO_2^-	1.00	1.00	1.00	1.00	1.00	0.00	1.00	1.00	0.00		n.s.	0.75	0.99
NO_3^-	0.00	0.00	0.00	1.00	1.00	1.00	0.14	0.00	1.00	1.00		n.s.	n.s.
N:P	1.00	1.00	1.00	1.00	1.00	0.00	1.00	1.00	0.00	0.03	1.00		0.83
Chl *a*	1.00	1.00	1.00	1.00	1.00	0.00	1.00	1.00	0.00	0.00	1.00	0.00	

Table S4. Spearman rank correlation coefficients (above the diagonal) and p-values (below the diagonal) of physicochemical paramters and Chl *a* for the DCM samples. Abbreviations are for latitude (Lat), temperature (Temp), vertical mixing coefficient (K_T), Brunt-Väisälä frequency (N^2) and nutrient flux into the euphotic zone (Z_{eu}*). n.s. indicates non-significance at $\alpha = 0.05$.

	Lat	Temp	Salinity	K_T	N^2	$Z_{eu}PO_4$	$Z_{eu}NO_3$	PO_4^{3-}	NH_4^+	NO_2^-	NO_3^-	N:P	Chl *a*
Lat		-1.00	-1.00	1.00	n.s.	n.s.	n.s.	1.00	n.s.	n.s.	1.00	n.s.	1.00
Temp	0.00		1.00	-1.00	n.s.	n.s.	n.s.	-1.00	n.s.	n.s.	-1.00	n.s.	-1.00
Salinity	0.00	0.00		-1.00	n.s.	n.s.	n.s.	-1.00	n.s.	n.s.	-1.00	n.s.	-1.00
K_T	0.00	0.00	0.00		n.s.	n.s.	n.s.	1.00	n.s.	n.s.	1.00	n.s.	1.00
N^2	1.00	1.00	1.00	1.00		n.s.	-1.00	n.s.	n.s.	-1.00	n.s.	-1.00	n.s.
$Z_{eu}PO_4$	1.00	1.00	1.00	1.00	1.00		n.s.	n.s.	-1.00	n.s.	n.s.	n.s.	n.s.
$Z_{eu}NO_3$	1.00	1.00	1.00	1.00	0.00	1.00		n.s.	n.s.	1.00	n.s.	1.00	n.s.
PO_4^{3-}	0.00	0.00	0.00	0.00	1.00	1.00	1.00		n.s.	n.s.	1.00	n.s.	1.00
NH_4^+	1.00	1.00	1.00	1.00	1.00	0.00	1.00	1.00		n.s.	n.s.	n.s.	n.s.
NO_2^-	1.00	1.00	1.00	1.00	0.00	1.00	0.00	1.00	1.00		n.s.	1.00	n.s.
NO_3^-	0.00	0.00	0.00	0.00	1.00	1.00	1.00	0.00	1.00	1.00		n.s.	1.00
N:P	1.00	1.00	1.00	1.00	0.00	1.00	0.00	1.00	1.00	0.00	1.00		n.s.
Chl *a*	0.00	0.00	0.00	0.00	1.00	1.00	1.00	0.00	1.00	1.00	0.00	1.00	

Table S5. Spearman rank correlation coefficients (above the diagonal) and p-vlaues (below diagonal) for abundances and mortality rates of microbial populations with biological and environmental parameters in the ML. Abbreviations are for vertical mixing coefficient (K_T), Brunt-Väisälä frequency (N^2), nutrient flux into the euphotic zone (Z_{eu}*), prokaryote (PA), viral (VA), virus to prokaryote ratio (VPR), heterotrophic nanaoflagellate abundance (HNF), prokaryotic production determined by leucine incorporation (PP_L) and with correction for loses (PP_{gross}), viral production (VP), protist mediated mortality (PMM), and the ratio of total mortality (TM) to PP_{gross}. n.s. indicates non-significance at $\alpha = 0.05$

	PA	VA	VPR	HNF	PP_L	PP_{gross}	Lytic VP	Prophage induction	Grazing rate	PMM	TM:PP_{gross}
Latitude	n.s.	0.93	n.s.	n.s.	1.00	n.s.	n.s.	n.s.	-0.89	n.s.	-0.81
Temperature	n.s.	-0.93	n.s.	n.s.	-1.00	n.s.	n.s.	n.s.	0.89	n.s.	0.81
Salinity	n.s.	-0.78	n.s.	n.s.	-0.94	n.s.	n.s.	n.s.	n.s.	n.s.	0.90
K_T	n.s.	n.s.	n.s.	n.s.	n.s.	n.s.	n.s.	n.s.	n.s.	n.s.	n.s.
N^2	n.s.	n.s.	n.s.	n.s.	n.s.	n.s.	n.s.	n.s.	n.s.	n.s.	n.s.
$Z_{eu}PO_4$	-0.77	n.s.	0.77	n.s.	n.s.	n.s.	n.s.	n.s.	n.s.	-0.89	n.s.
$Z_{eu}NO_3$	n.s.	n.s.	n.s.	n.s.	n.s.	n.s.	n.s.	0.85	n.s.	n.s.	n.s.
PO_4^{3-}	n.s.	n.s.	n.s.	n.s.	0.89	n.s.	n.s.	n.s.	n.s.	n.s.	-0.84
NH_4^+	n.s.	n.s.	-0.88	n.s.	n.s.	n.s.	n.s.	n.s.	n.s.	0.88	n.s.
NO_2^-	0.75	n.s.	n.s.	n.s.	n.s.	n.s.	n.s.	n.s.	n.s.	0.84	n.s.
NO_3^-	n.s.	n.s.	n.s.	n.s.	0.84	n.s.	n.s.	n.s.	n.s.	n.s.	-0.79
N:P	n.s.	n.s.	-0.94	n.s.	n.s.	0.77	0.83	n.s.	n.s.	0.89	n.s.
Chl *a*	0.77	n.s.	-0.77	n.s.	n.s.	n.s.	n.s.	n.s.	n.s.	0.89	n.s.
PA		0.75	n.s.	n.s.	n.s.	n.s.	n.s.	n.s.	n.s.	n.s.	n.s.
VA	0.03		n.s.	n.s.	0.93	n.s.	n.s.	n.s.	-0.99	n.s.	n.s.
VBR	1.00	1.00		n.s.	n.s.	n.s.	n.s.	n.s.	n.s.	-0.94	-0.75
HNF	1.00	1.00	1.00		n.s.	n.s.	n.s.	n.s.	n.s.	n.s.	n.s.
PP_L	1.00	0.00	1.00	1.00		n.s.	n.s.	n.s.	-0.89	n.s.	-0.81
PP_{gross}	1.00	1.00	1.00	1.00	1.00		0.94	n.s.	n.s.	n.s.	n.s.
Lytic VP	1.00	1.00	0.34	1.00	1.00	0.00		n.s.	n.s.	n.s.	n.s.
Prophage induction	1.00	1.00	1.00	1.00	1.00	1.00	1.00		n.s.	n.s.	n.s.
Grazing rate	0.09	0.00	1.00	1.00	0.00	1.00	1.00	1.00		n.s.	n.s.
PMM	1.00	1.00	0.00	1.00	1.00	0.34	1.00	1.00	1.00		n.s.
TM:PP_{gross}	1.00	0.42	0.03	0.75	0.00	1.00	1.00	1.00	0.50	0.14	

Table S6. Spearman rank correlation coefficients (above the diagonal) and p-vlaues (below diagonal) for abundances and mortality rates of microbial populations with biological and environmental parameters in the DCM. Abbreviations are for vertical mixing coefficient (K_T), Brunt-Väisälä frequency (N^2), nutrient flux into the euphotic zone (Z_{eu}*), prokaryote (PA), viral (VA), virus to prokaryote ratio (VPR), heterotrophic nanaoflagellate abundance (HNF), prokaryotic production determined by leucine incorporation (PP_L) and with correction for loses (PP_{gross}), viral production (VP), protist mediated mortality (PMM), and the ratio of total mortality (TM) to PP_{gross}. n.s. indicates non-significance at $\alpha = 0.05$ and NA indicates insufficient data

	PA	VA	VPR	HNF	PP_L	PP_{gross}	Lytic VP	Prophage induction	Grazing rate	PMM	TM:PP_{gross}
Latitude	n.s.	n.s.	n.s.	n.s.	n.s.	n.s.	n.s.	-1.00	n.s.	n.s.	n.s.
Temperature	n.s.	n.s.	n.s.	n.s.	n.s.	n.s.	n.s.	1.00	n.s.	n.s.	n.s.
Salinity	n.s.	n.s.	n.s.	n.s.	n.s.	n.s.	n.s.	1.00	n.s.	n.s.	n.s.
K_T	n.s.	n.s.	n.s.	n.s.	n.s.	n.s.	n.s.	-1.00	n.s.	n.s.	n.s.
N^2	n.s.	n.s.	1.00	n.s.	n.s.	n.s.	n.s.	n.s.	n.s.	1.00	n.s.
$Z_{eu}PO_4$	1.00	1.00	n.s.	n.s.	1.00	1.00	1.00	n.s.	-1.00	n.s.	n.s.
$Z_{eu}NO_3$	n.s.	n.s.	-1.00	n.s.	n.s.	n.s.	n.s.	n.s.	n.s.	-1.00	n.s.
PO_4^{3-}	n.s.	n.s.	n.s.	n.s.	n.s.	n.s.	n.s.	-1.00	n.s.	n.s.	n.s.
NH_4^+	-1.00	-1.00	n.s.	n.s.	-1.00	-1.00	-1.00	n.s.	1.00	n.s.	n.s.
NO_2^-	n.s.	n.s.	-1.00	n.s.	n.s.	n.s.	n.s.	n.s.	n.s.	-1.00	n.s.
NO_3^-	n.s.	n.s.	n.s.	n.s.	n.s.	n.s.	n.s.	-1.00	n.s.	n.s.	n.s.
N:P	n.s.	n.s.	-1.00	n.s.	n.s.	n.s.	n.s.	n.s.	n.s.	-1.00	n.s.
Chl *a*	n.s.	n.s.	n.s.	n.s.	n.s.	n.s.	n.s.	-1.00	n.s.	n.s.	n.s.
PA		1.00	n.s.	n.s.	1.00	1.00	1.00	n.s.	-1.00	n.s.	n.s.
VA	0.00		n.s.	n.s.	1.00	1.00	1.00	n.s.	-1.00	n.s.	n.s.
VBR	1.00	1.00		n.s.	n.s.	n.s.	n.s.	n.s.	n.s.	1.00	n.s.
HNF	1.00	1.00	1.00		n.s.	n.s.	n.s.	n.s.	n.s.	n.s.	NA
PP_L	0.00	0.00	1.00	1.00		1.00	1.00	n.s.	-1.00	n.s.	n.s.
PP_{gross}	0.00	0.00	1.00	1.00	0.00		1.00	n.s.	-1.00	n.s.	n.s.
Lytic VP	0.00	0.00	1.00	1.00	0.00	0.00		n.s.	-1.00	n.s.	n.s.
Prophage induction	1.00	1.00	1.00	1.00	1.00	1.00	1.00		n.s.	n.s.	n.s.
Grazing rate	0.00	0.00	1.00	1.00	0.00	0.00	0.00	1.00		n.s.	n.s.
PMM	1.00	1.00	0.00	1.00	1.00	1.00	1.00	1.00	1.00		n.s.
TM:PP_{gross}	1.00	1.00	1.00	NA	1.00	1.00	1.00	1.00	1.00	1.00	

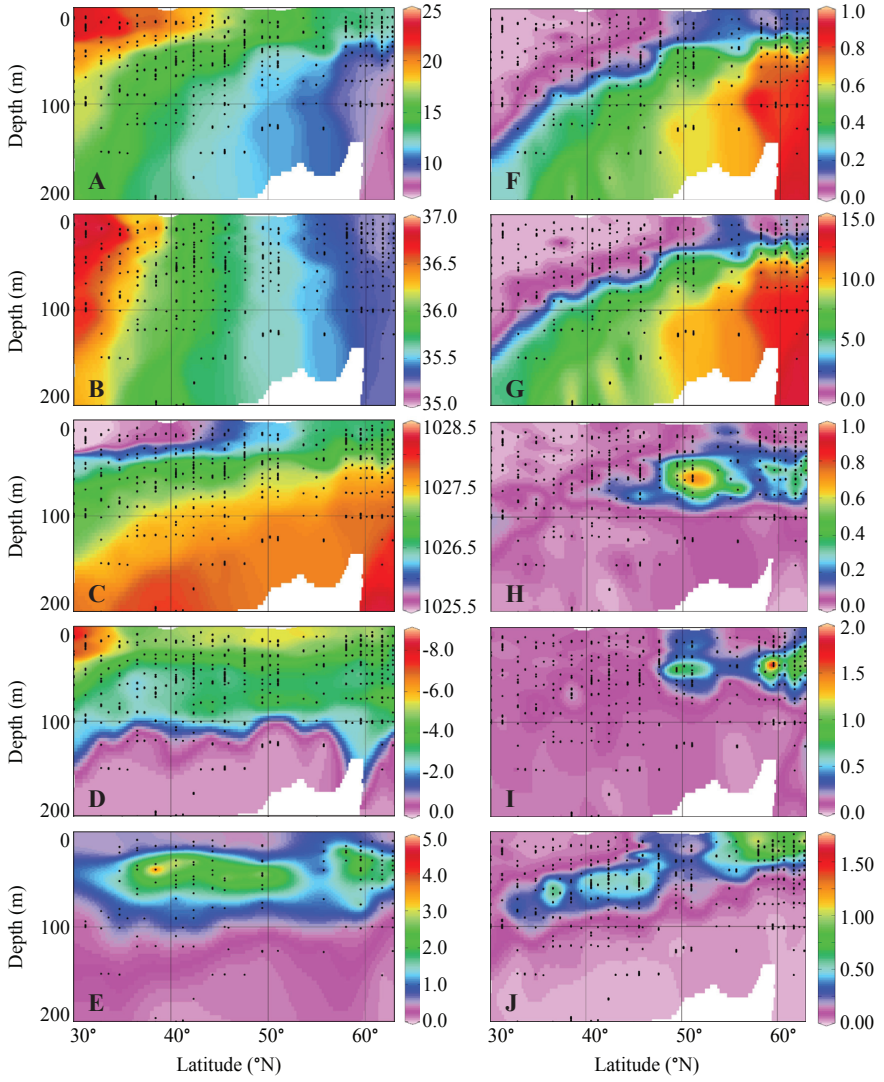

Figure S1. Latitudinal and depth distribution of (**A**) temperature (°C), (**B**) salinity, (**C**) density (kg m^{-3}), (**D**) $\log(K_T)$ (m^2 s^{-1}), (**E**) Brunt-Väisälä frequency, N^2 ($x10^{-4}$ rad^2 s^{-2}), (**F**) inorganic phosphate (µM), (**G**) nitrate (µM), (**H**) nitrite (µM), (**I**) ammonia (µM) and (**J**) Chl *a* autofluorescence (µg Chl *a* l^{-1}) measured during STRATIPHYT. Black dots indicate sampling points. Figure panels were prepared using Ocean Data View version 4 (Schlitzer 2002).